Proc. Natl. Acad. Sci. USA
Vol. 96, pp. 8332–8333, July 1999
From the Academy

This paper is a summary of a session presented at the fourth annual German-American Frontiers of Science symposium, held June 4–6, 1998, at the Arnold and Mabel Beckman Center of the National Academies of Sciences and Engineering in Irvine, CA.

The mathematics of microstructure and the design of new materials

K. BHATTACHARYA*, G. FRIESECKE†, AND R. D. JAMES‡§

*Division of Engineering and Applied Science, California Institute of Technology, Pasadena, CA 91125; ‡Mathematical Institute, University of Oxford, Oxford OX1 3LB, United Kingdom; and ‡Department of Aerospace Engineering and Mechanics, University of Minnesota, Minneapolis, MN 55455

The "pathological" energy function $E(u) = u^2$ for $u \neq 0, E(0) = 1$, has no minimizer. As u decreases to 0, the energy also decreases, but there is no way to achieve the value 0. Although examples like this might seem to be unimaginably far from scientific thought, they are at the heart of a new approach (1) to understand the complex microstructure and macroscopic response of materials that undergo phase transformations. The free energy of such materials typically has no minimizer, and the observed microstructures (complex, fine-scale patterns of domains of different atomic lattice structure as shown below in a micrograph of CuAlNi by C. Chu and R.D.J.; Fig. 1) have their origin in the material's ultimately futile attempt to find the minimum energy state (2).

The lack of a ground state prohibits prediction of the macroscopic response from microscopic data via the standard procedure: determine the free energy, find the minimizing state, and evaluate its macroscopic properties. Emerging mathematical methods, linked to profound work in the 1940s by L. C. Young and recently surveyed in (3), nevertheless deliver well defined macroscopic quantities, obtained via averaging over all low-energy states. One area where predictions obtained in this new way have played a role is the recent synthetization of a new magnetostrictive material (4, 5) whose magnetostrictive strain is 50 times larger than that of giant magnetostrictive materials (formerly those with the largest strain).

Energy Functions and Energy Wells. The materials on which the new coarse-graining methods have been brought to bear are alloys exhibiting a martensitic transformation. In this transformation, below a critical temperature, the unit cell of the crystal undergoes a bifurcation into different, lower symmetry unit cells. (Not just thousands of alloys but also ceramics and proteins undergo this transformation.) The relevant microscopic parameters (transition temperature, symmetry changes, and lattice parameters) can be regarded as known from atomic measurements and can be subsumed into a cell energy function $\Phi(F, \theta)$ depending on temperature and on the 3×3 matrix $F = (e_1, e_2, e_3)$ of lattice vectors of the cell. A macroscopic sample can be described by a continuous vector field $y(x)$ indicating the position of the lattice site formerly at x (martensitic transformations are coherent, i.e., the atomic bonds stay intact). The complicated cooperative effects between the cells, which result in structures like the one shown above, can be explained via minimization of the total free energy (1)

$$E = \int_\Omega \Phi\left(\frac{\partial y}{\partial x_1}, \frac{\partial y}{\partial x_2}, \frac{\partial y}{\partial x_3}, \theta\right) dx\,,$$

where x varies over the specimen Ω. (Think of the integral as a sum over unit cells with corner x and of the derivatives $\frac{\partial y}{\partial x_i}$ as the corresponding lattice vectors.) The cell energy Φ is minimized on those triples F of lattice vectors that correspond to the stable unit cells at temperature θ. Typically, there is only one stable cell or "energy well" at high temperatures (Fig. 2 *Upper Left*) and many at low temperatures (Fig. 2 *Lower Left*). For example, for a cubic-to-tetragonal transformation as in InTl, the high-temperature well is of the form $F = RI$ where $I = diag(1, 1, 1)$ and R is a rotation (note: rotations leave the free energy invariant). This well is shown as the dashed circle in Fig. 2 *Right*. Below the transition temperature, there are three wells, shown as solid circles, which correspond to elongation of the unit cell along either of the three crystallographic axes and are given by $RU_1 = R\,diag(\eta_1, \eta_2, \eta_2)$, $RU_2 = R\,diag(\eta_2, \eta_1, \eta_2)$, and $RU_3 = R\,diag(\eta_2, \eta_2, \eta_1)$ where the η_i are the transformation stretches.

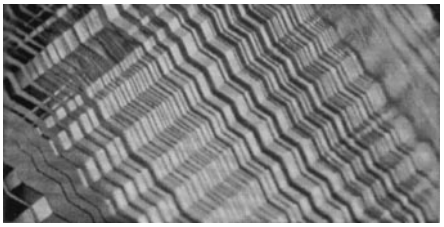

FIG. 1. Typical microstructure of CuAlNi.

From Energy Wells to Nonattainment. Whereas Φ is a function of unit cells, i.e., a nine-dimensional energy landscape, E is a function of patterns y, i.e., an infinite-dimensional energy landscape. Depending on applied fields and loads, minimizing patterns can be highly complex or may in fact not exist at all, despite the simple-looking formula for E. It is instructive (6) to reduce to one deformation component $y(x_1, x_2)$ depending on two spatial variables, and to consider the case of two wells $\Phi = ((\partial y/\partial x_1)^2 - 1)^2 + ((\partial y/\partial x_2)^2)$ and of four wells $[\Phi = ((\partial y/\partial x_1)^2 - 1)^2 + ((\partial y/\partial x_2)^2 - 1)^2]$. The behavior of the total free energy $E = \int_0^1 \int_0^1 \Phi(\partial y/\partial x_1, \partial y/\partial x_2)\, dx$ depends in a spectacular way on the linear deformation $y(x) = Fx$ prescribed on the boundary (6). The boundary condition, which idealizes a hard loading device, enforces the average strain F, in competition with the locally preferred strains $(\pm 1, 0)$ in the two-well case (Fig. 3 *Left*) and $(\pm 1, \pm 1)$ in the four-well case (Fig. 3 *Right*). If $F = (F_1, F_2)$ lies in the white parameter region, the energy is minimized by the homogeneous deformation $y(x) = Fx$. In the lightly shaded region, the energy is minimized by a heterogeneous state. In the dark region, there is no minimizer, finer and finer microstructure being necessary to lower the energy. [Other natural examples of nonattainment arise e.g., in quantum chemistry or optimal control problems (7).]

Coarse-Graining in Case of Nonattainment. If the energy function E exhibits nonattainment, the mathematical object replacing a minimizing deformation $y(x)$ is a probability distribution

Abbreviation: SME, shape-memory effect.

§To whom reprint requests should be addressed. e-mail: james@aem.umn.edu.

PNAS is available online at www.pnas.org.

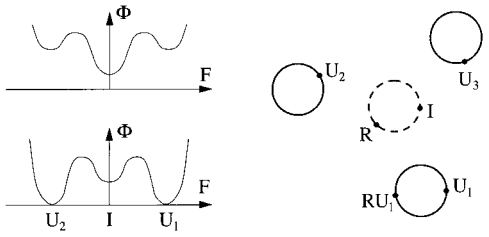

FIG. 2. Multiwell energy.

ν_x of values of the deformation gradient $Dy(x)$ (called Young measure) obtained by averaging over low-energy states (8). For the two-well example (see above) with $F = 0$, the optimal distribution is $Dy(x) = (1, 0)$ and $Dy(x) = (-1, 0)$ with equal probability 1/2, representing physically a microstructure of 50 percent of each phase. (Ongoing research on such "generalized solutions" of minimization problems is described in (3). Macroscopic quantities are obtained by taking expected values, e.g., the macroscopic energy density is the expected value of $\Phi(Dy(x), \theta)$.

A fascinating and largely unresolved area is that of kinetic response. It was found recently that a wealth of nonminimizing patterns enjoy unexpected long-time stability under small perturbations (9), whereas it had been shown earlier how the assumption of many metastable states implies a novel macroscopic kinetic law different from that obtained by averaging the underlying energy surface (10). An instructive example is a simple quadratic energy with superimposed small wiggles of length scale ε, $E_\varepsilon(u) = u^2/2 + a\varepsilon \sin(u/\varepsilon)$, on which we let a particle move by steepest descent kinetics $\dot{u}_\varepsilon(t) = -E_\varepsilon'(u(t))$ (10). Averaging out the wiggles of the energy surface leads to the energy $\lim_{\varepsilon \to 0} E_\varepsilon(u) = E(u) = u^2/2$ and the kinetic law $\dot{u}(t) = -E'(u(t))$, which is incorrect. The correct macroscopic law is $\dot{u}(t) = \sqrt{u^2 - a^2}$ for $u \leq -a$, $\dot{u}(t) = 0$ for $-a < u < a$, and $\dot{u}(t) = -\sqrt{u^2 - a^2}$ for $u \geq a$.

Predictions About Shape-Memory Alloys. Some martensitic materials display the amusing and useful shape-memory effect (SME), where a material subjected to severe deformation below a critical temperature jumps back to its original shape on heating. But not all martensites display this phenomenon. Why? Simply stated, the SME requires some very special microstructural features and this in turn requires that the energy wells be arranged in a very special manner. The methods described above have been used to turn this idea into explicit criteria: the SME requires that the transformation stretches (like η_1, η_2 above) satisfy an explicitly known but very restrictive condition and the high temperature phase have cubic crystallographic symmetry (11, 12). Furthermore, the extent of the SME depends on the way the specimen is created. Many alloys display the SME as carefully prepared single-crystal specimens; however, only TiNi displays a large SME in commercially prepared wires, tubes, and strips. The latter specimens are polycrystals, composed of innumerable small single crystals or grains with possibly differing orientation. It turns out that the grains behave in a most uncooperative manner and destroy any SME unless the low-temperature phase has small crystallographic symmetry (13) and the texture

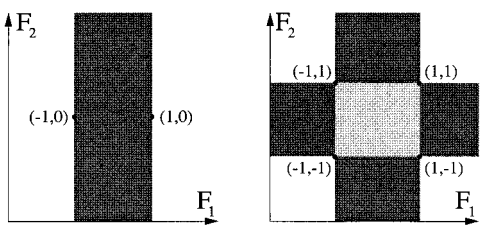

FIG. 3. Attainment/nonattainment diagram.

(the size, shape, and orientation of grains) is just right. The first requirement dooms virtually all materials except TiNi and some Cu-based alloys like CuZnAl and CuAlNi, and the second requirement dooms the Cu-based alloys when made as wires, tubes, and strips (13, 14).

Current interest in micromachines has inspired many experimental efforts to make thin-film shape-memory materials, and most of these have concentrated on TiNi with limited success. A recent calculation shows that two common ways of making these films, sputtering and meltspinning, produce undesirable texture in TiNi. A better alternative is to make the (previously condemned) Cu-based alloys by meltspinning (13). Finally, theory has also pointed out the great potential of single-crystal thin films and proposed novel designs of micropumps (15, 16). Thus, these theoretical methods provide a road map for materials selection and design.

New Materials. The typical procedure in science, explained above, is to begin from the real material, describe its energy-well structure, find minimum energy states, predict the microstructure and, in some cases, the material behavior, and then compare with experiment. But theory can also be used in an inverse way. We begin with a theoretical concept of an interesting property or effect, formulate a hypothetical energy-well structure that produces this effect via energy minimization or the solution of a dynamic theory, propose a hypothetical material, then go to the laboratory and actually make the material. The inverse procedure is one of the most exciting for theory, and for materials science, as it can lead to an entirely new material that might not have been anticipated by purely experimental approaches.

The inverse procedure has been followed for the development of new "ferromagnetic shape-memory" materials (4), materials that combine ferromagnetism and shape-memory. The free energies of such materials are sensitive to deformation (through the deformation gradient), magnetization, and temperature. As the temperature is decreased, they exhibit a set of energy wells associated with a ferromagnetic transition; with a further decrease in temperature these are joined by another set of wells associated with a martensitic transformation. All of these wells live on a complex 12-dimensional energy landscape, which, however, is precisely restricted by conditions of symmetry and rotational invariance. The central question for ferromagnetic shape memory is "What energy-well structures lead to a large change of macroscopic shape when a magnetic field is applied to the specimen?" An analysis of this question, and its application to a program of alloy development, have now produced materials that exhibit, under moderate field, about 50 times the field-induced strain of giant magnetostrictive materials. Until some 6 months before this Symposium, giant magnetostrictive materials exhibited the largest strain known.

1. Ball, J. M. & James, R. D. (1987) *Arch. Rat. Mech. Analysis* **100,** 13–52.
2. Ball, J. M. & James, R. D. (1992) *Phil. Trans. R. Soc. London A* **338,** 389–450.
3. Müller, S. (1998) in *Proceedings of C. I. M. E. Summer School Cetraro 1996*, eds. Hildebrandt, S. & Struwe, M. (Springer, Berlin), in press.
4. James, R. D. & Wuttig, M. (1998) *Phil. Mag. A* **77,** 1273–1299.
5. Tickle, R. James, R. D., Shield, T., Schumacher, P., Wuttig, M. & Kokorin, V. V. (1999) *IEEE Trans. Magn.*, in press.
6. Friesecke, G. (1994) *Proc. Roy. Soc. Edinb.* **124A,** 437–471, 1994.
7. Young, L. C. (1960) *Lectures on the Calculus of Variations and Optimal Control Theory* (Chelsea, New York).
8. Ball, J. M. (1989) in *Springer Lecture Notes in Physics*, eds. Rascle, M., Serre, D. & Slemrod, M. (Springer, Berlin), Vol. 3, pp. 207–215.
9. Friesecke, G. & McLeod, J. B. (1997) *Proc. R. Soc. London Ser. A* **453,** 2427–2436.
10. Abeyaratne, R., Chu, C. & James, R. D. (1996) *Phil. Mag. A* **73,** 457–497.
11. Bhattacharya, K. (1991) *Acta Mat. Mater.* **39**, 2431–2444,
12. Bhattacharya, K. (1991) *Arch. Rat. Mech. Anal.* **39,** 2431–2444.
13. Bhattacharya, K. & Kohn, V. (1996) *Acta Mater.* **44,** 529–542.
14. Bhattacharya, K. & Kohn, V. (1997) *Arch. Rat. Mech. Anal.* **139,** 99–180.
15. Shu, Y. C. & Bhattacharya, K. (1999) *Acta Mater.*, in press.
16. Bhattacharya, K. & James, R. D. (1999) *J. Mech. Phys. Solids* **47,** 531–536.